Fossil genes and microbes in the oldest ice on Earth

Kay D. Bidle*, SangHoon Lee*†, David R. Marchant‡, and Paul G. Falkowski*§¶

*Environmental Biophysics and Molecular Ecology Program, Institute of Marine and Coastal Sciences, and §Department of Geological Sciences, Rutgers, The State University of New Jersey, New Brunswick, NJ 08901; †Polar Research Institute, Korea Ocean Research and Development Institute, Incheon 406-840, Korea; and ‡Department of Earth Sciences, Boston University, Boston, MA 02215

Edited by David M. Karl, University of Hawaii, Honolulu, HI, and approved June 26, 2007 (received for review March 9, 2007)

Although the vast majority of ice that formed on the Antarctic continent over the past 34 million years has been lost to the oceans, pockets of ancient ice persist in the Dry Valleys of the Transantarctic Mountains. Here we report on the potential metabolic activity of microbes and the state of community DNA in ice derived from Mullins and upper Beacon Valleys. The minimum age of the former is 100 ka, whereas that of the latter is ≈8 Ma, making it the oldest known ice on Earth. In both samples, radiolabeled substrates were incorporated into macromolecules, and microbes grew in nutrient-enriched meltwaters, but metabolic activity and cell viability were critically compromised with age. Although a 16S rDNA-based community reconstruction suggested relatively low bacterial sequence diversity in both ice samples, metagenomic analyses of community DNA revealed many diverse orthologs to extant metabolic genes. Analyses of five ice samples, spanning the last 8 million years in this region, demonstrated an exponential decline in the average community DNA size with a half-life of ≈1.1 million years, thereby constraining the geological preservation of microbes in icy environments and the possible exchange of genetic material to the oceans.

ancient ice | community DNA | metabolism | metagenomic analysis | cosmic radiation

Antarctica offers unique environments for understanding the limits of biological metabolism and geological preservation of life and genetic material. Analyses of microorganisms in subglacial lakes, including Lake Vostok (1) and Lake Bonney (2), as well as the Taylor Dome region of the Transantarctic Mountains (3), have revealed the potential viability of microorganisms preserved in ice up to ≈300 ka. In the Dry Valleys of the Transantarctic Mountains, however, patches of much older ice persist, yet little is known about the viability of microbes or the state of genetic material in these regions.

Here we report on the microbial activity and state of the community DNA in samples from a debris-covered alpine glacier that heads in Mullins Valley (sample no. DLE-98-12) and terminates along a diffuse boundary in Beacon Valley (sample no. EME-98-03) (Fig. 1 *A* and *B*). Synthetic aperture-radar interferometry analysis indicated that ice within Mullins Valley ranges from modern at the valley head to ≈300 ka near the tributary mouth, whereas buried ice on the floor of upper and central Beacon Valley could be as much as 10 Ma (4). DLE-98-12, which is assigned an age of ≈100 ka, lies halfway down Mullins Valley, whereas EME-98-03 lies in the zone estimated to be up to 8 Ma (Fig. 1*A*). These ice chronologies are supported by ^{3}He and ^{21}Ne cosmogenic dating of surface boulders (5) and laser-fusion ^{40}Ar/^{39}Ar radiometric dating of surface ash-fall deposits (6, 7) [supporting information (SI) *Text*]. Analyses of the ice crystal structure and stable-isotope composition (δ^{18}O, δD) indicate that the ice samples have remained frozen since transformation from snow to glacier ice (e.g., refs. 6 and 7). There were also no detectable cryoconite holes in the glacier surface or morphologic evidence of past meltwater formation at these sample locations. Hence, all data pertaining to the age of the Mullins Valley debris-covered glacier are internally consistent and suggest that microorganisms and DNA in the ice at EME-98-03 and DLE-98-12 have been encased since the late Miocene and mid-Pleistocene, respectively.

Results and Discussion

DLE-98-12 and EME-98-03 contained a broad size spectrum of particles and rock debris, ranging from fine silt to coarse sand, which likely originated from rockfall (sandstone and dolorite) onto the ice accumulation zone. These inorganic particles contributed to variations in chemical properties and microzones within and between the meltwater samples (2) (SI Table 1). For example, meltwater of EME-98-03 was pH 6.9, whereas that from DLE-98-12 was pH 4, due to the chemical reactions of, e.g., pyrite in the latter. SEM of DLE-98-12 revealed the presence of distinct coccoid particles, suggestive of intact microbes, interspersed with mineral granules (Fig. 1*C*, arrows). SEM analysis of EME-98-03 revealed a much higher fine-particle load along with abundant sheath-like filaments, which were evenly distributed throughout the sample (Fig. 1*D*). Staining with SYBR gold (Fig. 1 *E* and *F*) indicated that microbial concentrations were 5.07 ($\pm$0.98) $\times$ 10^5 and 3.28 ($\pm$1.56) $\times$ 10^4 cells per ml^{-1} for DLE-98-12 and EME-98-03, respectively. These values are comparable to those from polar freshwater (8, 9) and sea ices (10) but are 2–3 orders of magnitude higher than in Antarctic snow (11) and subglacial lake ice accretions (1).

To more fully understand the microbial composition of the two ice samples, we amplified community DNA (Fig. 2) and constructed clone libraries with *Bacteria*-specific 16S rDNA primers (SI Table 2 and SI Fig. 6). Repeated attempts to amplify community DNA with *Archaea*- and *Eukaryotic*-specific primers were unsuccessful, as were attempts to amplify MilliQ (Millipore, Billerica, MA) rinse water. Both EME-98-03 and DLE-98-12 were dominated by relatively few bacterial phylotypes (SI Table 2 and SI Fig. 6). After removal of potential chimeric sequences (n = 36) and dereplication of identical sequences, 30 distinct phylotypes (11 from 96 EME clones, and 19 from 123 DLE clones) were identified. BLAST analysis of the 30 phylotypes (SI Table 2) revealed no identical clones to 16S rDNA sequences in GenBank, with several having reduced phylogenetic similarity (<95%) to currently catalogued species. Overall, the EME-98-03 clone library had a low diversity, largely dominated by one phylotype of β-proteobacteria (Group A1, EME076; 62 of 96 clones) (SI Table 2). The remaining sequences belonged to γ-proteobacteria, α-proteobacteria, *Acidobacteria*, *Firmicutes*, and *Cytophaga-Flavobacterium-Bacteroides* (CFB) divisions, each occurring at lower frequencies. A majority of EME-98-03 clones (68 of 96) returned BLAST matches with ≥98% identity to *Leptothrix sp.* (EME076; 99% identity), a representative

Author contributions: K.D.B. and S.L. contributed equally to this work; K.D.B., S.L., and P.G.F. designed research; K.D.B. and S.L. performed research; K.D.B., S.L., and D.R.M. contributed new reagents/analytic tools; K.D.B., S.L., D.R.M., and P.G.F. analyzed data; and K.D.B., S.L., D.R.M., and P.G.F. wrote the paper.

The authors declare no conflict of interest.

This article is a PNAS Direct Submission.

Freely available online through the PNAS open access option.

Abbreviation: PC, polycarbonate.

Data deposition: The sequences reported in this paper have been deposited in the GenBank database (accession nos. ER915562–ER916102; ER916113; EF127594–EF127627).

¶To whom correspondence should be addressed. E-mail: falko@marine.rutgers.edu.

This article contains supporting information online at www.pnas.org/cgi/content/full/0702196104/DC1.

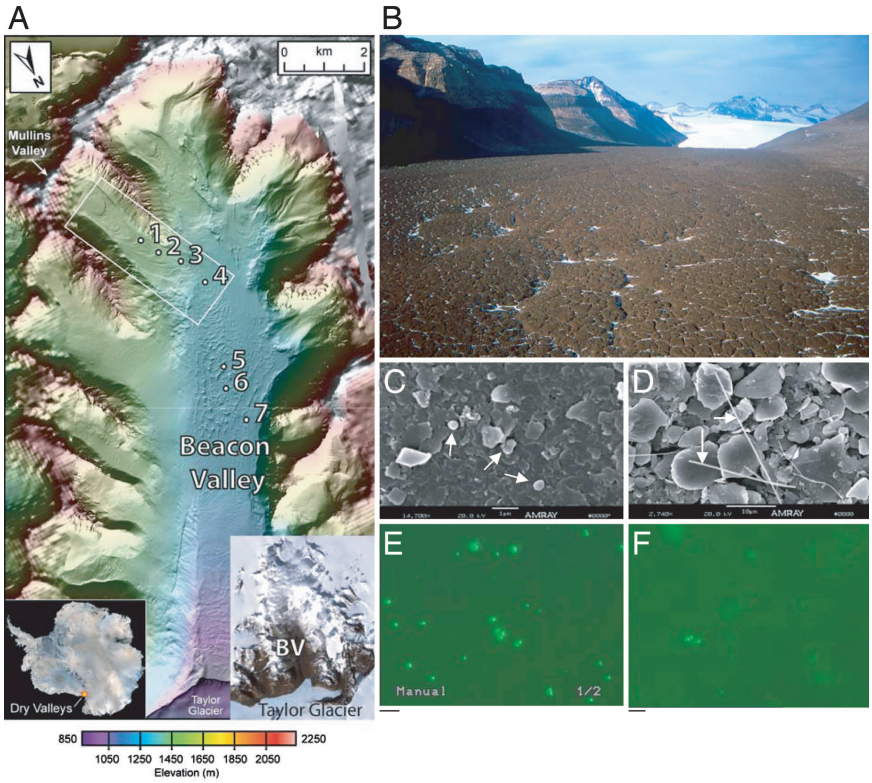

Fig. 1. Geologic setting of buried ice from Mullins and Beacon Valleys and evidence of encased microbes. (*A*) Digital elevation model showing the distribution of ice samples collected at various locations in Mullins (white box) and Beacon Valleys. Ice between locations marked one and seven spans an ≈8 million-year transect (1, DLE-98-12, ≈100 ka; 2, DLE-98-11, ≈200 ka; 3, DLE-98-CS-1, ≈300 ka; 4, MCI-04-013, ≈2 Ma; 5, EME-98-08, ≈5–6 Ma; 6, EME-98-01, ≈6–7 Ma; 7, EME-98-03, ≈8 Ma). (*Inset Left*) Location of the Dry Valleys in relation to the Antarctic continent; (*Inset Right*) Overview of Beacon Valley and nearby Taylor Glacier. (*B*) Photograph of Beacon Valley with view to the northeast toward Taylor Glacier. (*C* and *D*) Scanning electron micrographs and (*E* and *F*) epifluorescence micrographs of ice samples from DLE-98-12 (*C* and *E*) and EME-98-03 (*D* and *F*), illustrating DNA-containing bacteria cells and their morphology compared with glacial till. DLE-98-12 possessed cocci-like cells scattered among mineral debris (arrows), whereby EME-98-03 had filamentous sheath-like structures.

of the sheathed, filamentous bacteria (12), and consistent with SEM observations (Fig. 1*D*). Similar representatives of sheathed bacteria, such as *Leptothrix lopholea*, have also been recovered from Greenland and Antarctic ice cores ranging from 0.5 to 400 ka (13). The DLE-98-12 clone library was dominated by phylotypes of *Acidobacteria* (96 of 123 clones), followed by a single phylotype of α-proteobacteria (17 of 123 clones), and both *Actinobacteria* and CFB phylotypes in lower frequencies. No DLE clones were similar to any known sequences at the species level (≥98% identity).

To examine whether the microorganisms encased in these two ice samples were metabolically active, we measured the incorporation of ^{3}H-leucine and ^{3}H-thymidine into protein and nucleic acid pools, respectively, and followed the incorporation and subsequent respiration of ^{14}C-glucose. Although radiotracer incorporation was variable, metabolic activity was readily detected in both samples after correcting with formalin-killed controls (Fig. 3 *A* and *B*; SI Table 3). Overall, DLE-98-12 meltwater displayed more extensive ^{3}H-leucine and ^{14}C uptake, as well as ^{14}C respiration, compared with the older ice. EME-98-03 had high ^{3}H-thymidine uptake, whereas ^{3}H-leucine uptake was indistinguishable from formalin-killed controls. In general, the rates of ^{14}C incorporation were low relative to ^{14}C respiration, suggesting the microbes were not in balanced growth under these conditions. The uptake signal from MilliQ rinse water was also indistinguishable from controls. Nutrient augmentation of meltwaters stimulated earlier and greater radiotracer incorporation into macromolecules (SI Table 3).

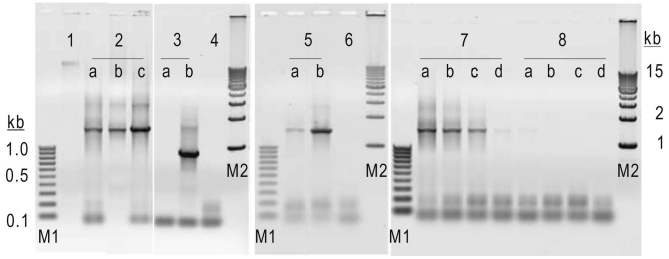

Fig. 2. PCR amplification of encased microbial community DNA. Lane 1, environmental DNA from DLE-98-12 ice meltwater; lane 2, *Bacteria*-specific 16S rDNA PCR amplicons for DLE-98-12 (2a, raw; 2b, gel purified) and *E. coli* (2c, +control); lane 3, *Archaea*-specific 16S rDNA PCR amplicons for DLE-98-12 DNA (3a) and *Haloferax volcanii* (3b, +control); lanes 4 and 6 correspond to PCR reagent negative controls. Lane 5, *Bacteria*-specific 16S rDNA PCR amplicons for EME-98-03 (5a) and *E. coli* (5b, +control). Lane 7, *Bacteria*-specific 16S rDNA PCR amplicons for DLE-98-12 with DNA template serially diluted ×1 (7a), ×5 (7b), ×25 (7c), and ×125 (7d). Lanes 8a–8d, same as lane 7 but for the MilliQ water contamination control. Ice DNA template was routinely diluted (>×10) for PCR amplification. M1 and M2, molecular weight ladders with 0.1- and 1-kb increments, respectively.

Long-term incubation of nutrient-amended meltwater at 4°C in the dark resulted in the recovery of viable cells from both ice samples (Fig. 3 *C* and *D*; SI Table 3). In contrast, MilliQ-inoculated controls showed no detectable growth. For DLE-98-12, two of the nutrient-amended samples (T1 and T4) showed relatively rapid growth (≈7-d doubling time), from which we obtained 16S rDNA amplicons (Fig. 2*F*) and isolated viable colonies on plate media (Fig. 2*E*), both of which were identified as *Arthrobacter* sp. via 16S rDNA sequencing (SI Table 4). Their presence in the initial ice microbial community was verified by nested PCR whereby isolate-specific 16S rDNA primer sets successfully amplified the original 16S rDNA amplicons as template (Fig. 3*F*). Interestingly, the 16S rDNA sequence from one isolate (DLE011) was a 99% match to *Arthrobacter roseus* (accession no. AJ278870), which had previously been isolated from a cyanobacterial mat in the Wright Valley, ≈30 km from the DLE-98-12 sample site (14). Nutrient amended EME-98-03 meltwaters displayed extremely slow, low-level growth with apparent doubling times of 30–70 d (Fig. 3*D*), which was confirmed by epifluorescence microscopy. Unfortunately, repeated attempts to recover viable cells from EME-98-03 on solid media and to determine their identity via PCR amplification consistently failed. The extremely slow and low-level growth, combined with the inability to recover viable cells, suggests that a subset of microbes

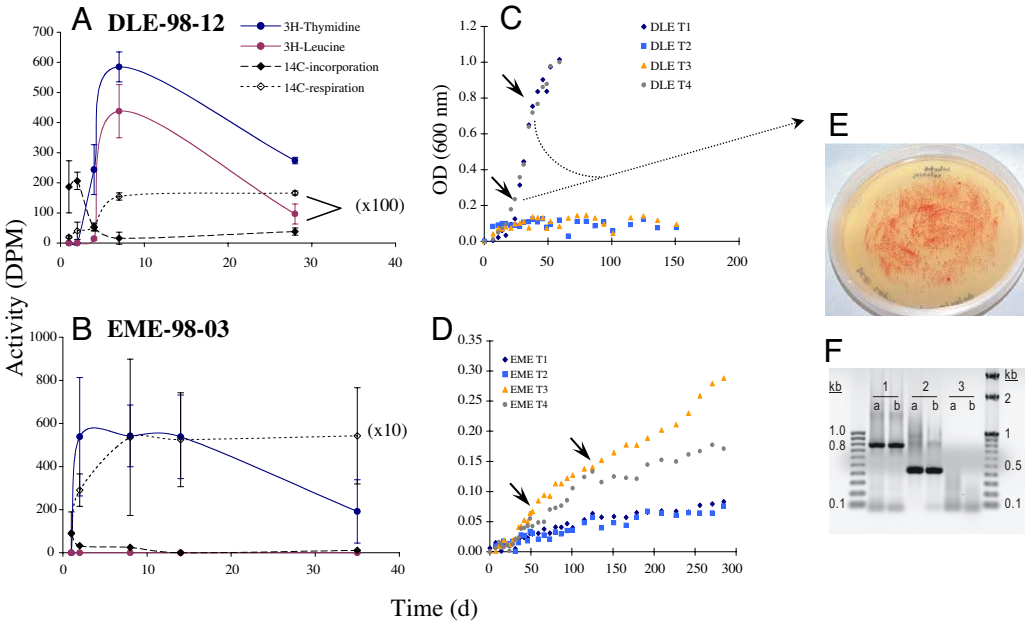

Fig. 3. Assessment of the metabolic activity and viability of microorganisms encased in DLE-98-12 and EME-98-03. (*A* and *B*) Incorporation and respiration of ^{3}H-thymidine, ^{3}H-leucine, and ^{14}C-glucose in ice-meltwater samples during incubation at 4°C. Data are corrected for formalin-killed controls. Note different scales for ^{3}H-leucine incubation in *A* and ^{14}C-respiration in *A* and *B*. Error bars represent standard deviation among replicate incubations. (*C* and *D*) Time course of viable cell growth in nutrient supplemented ice-water cultures. Note the differences in scales, reflecting dramatic growth discrepancies between DLE-98-12 and EME-98-03. Symbols refer to the ice (DLE or EME) and nutrient type (T1–T4). Arrows indicate time points when subsamples were removed and used for PCR amplification of *Bacteria*-specific 16S rDNA and plating onto solid media (*E*). Amplification and colony formation were successful only for DLE cultures with recovered phylotypes given in SI Table 4. (*F*) Nested PCR amplification verified the presence of cultured isolates in the original ice microbial community. DLE011i/*A. roseus* CMS90 and *Arthrobacter* sp. primer sets produced their expected ≈770- and ≈440-bp fragment sizes, respectively, using both community *Bacterial* 16S rDNA amplicons (lanes 1a and 2a) and DLE011i genomic DNA (lanes 1b and 2b, +control) as template. *E. coli* genomic DNA (lanes 3a and 3b) was used as a negative control for both primer sets.

encased in ice for 8 million years are viable, but their viability is seriously compromised. The correspondence between bacterial 16S rDNA phylotypes, meltwater chemistry, and SEM observations, as well as the failure to recover PCR amplicons or viable cells from 0.22-μm filtered MilliQ water used to ablate the ice before sampling for microbes and DNA, strongly argues against contamination artifacts.

Assuming the age model for these ice samples is correct, the encased DNA is literally a gene bank, with deposits made when the ices formed. Our 16S rDNA analyses suggest that deposits were made from aeolian fluxes of exogenous microbes (15, 16) and from endogenous glacial till (SI Table 2). To examine the integrity of encased DNA in these ice samples, we analyzed the size of the extracted community genomic DNA using agarose gel electrophoresis. DNA from DLE-98-12 migrated as a tight band at ≈20 kb, whereas that from EME-98-03 was a broad smear of much lower molecular weight fragments (100-<1,000 bp), indicative of extensive degradation (Fig. 4). We calculated the weighted mean size of the extracted genomic DNA to be 18,500 bp for DLE-98-12 and 210 bp for EME-98-03. Electrophoretic analyses of DNA extracted from additional ice samples from this region (DLE-98-CS-1, ≈300 ka; MCI-04-13, ≈3 ± 1 Ma; and EME-98-8, 5–6 Ma; Fig. 1*B*) also revealed time-dependent DNA degradation that follows pseudofirst-order kinetics with a half-life of ≈1.1 Ma (Fig. 4). This degradation rate is generally consistent with calculations of DNA survival and depurination rates, where an average bacterial genome (3×10^6 bp) would be broken into ≈100-bp fragments in >1.2 Ma at temperatures below −20°C (17). The possibility that these dramatic differences in DNA size resulted from shearing can be ruled out; all ice samples were processed identically. The progressive change in DNA size suggests that the buried ice has not undergone melting in the recent geologic past and could not have formed as segregation ice by the *in situ* freezing of surface meltwater.

The primary cause of DNA degradation is unknown. One possibility is hydrolysis and/or oxidation by hydroxyl ion or proton attack on the sugar backbone or glycosidic bonds (depurination/depyrimidination) (17–19). This hypothesis is not supported by the chemical data; the younger, more acidic ice follows the same degradation pattern as older, neutral pH ice (Fig. 4). A second possibility is the generation of ionizing radiation from cosmic high-energy particles (e.g., μ-muons and/or protons). Because of the Compton effect (20), Antarctica receives among the highest amount of incoming cosmic radiation on the planet (21). Given a target size of ≈10–20 Å^2 for a covalent bond along the phosphosugar backbone, a minimum of 14 ionizing events is required to reduce the DNA from ≈3 Mbp to ≈210 bp over the 8 million-year interval. Assuming the integrated cosmic flux is relatively constant over geological time (i.e., magnetic reversals are relatively short-term events in this context), and ignoring the upward migration of ice samples during sublimation toward higher cosmic fluxes nearer the ground surface (5), target theory predicts that a cosmic radiative flux of four to six particles cm^{-2}·s^{-1} is required to support this degradation rate of DNA, well within the bounds of the present flux. The considerable degradation in EME-98-03 and its consistency with the DNA "kill curve" relationship argues against a time-dependent increase in the frequency of intermolecular/interstrand cross-linking, which serve to stabilize the DNA and reduce fragmentation (17). Our analysis suggests that a DNA-size model can be used as a geomolecular proxy to independently estimate ice age in this region.

Resuscitation of microbes from both ice types raises the question of whether the encased microbes have been preserved in an inactive state for their respective time periods, or were capable of *in situ* maintenance metabolism. The absence of data for cryoconite holes and meltwater formation argue for long-term preservation in these ice samples. However, liquid water can exist in ice as microlayers around sediment grains or as microdiameter veins caused by ionic impurities in the crystal structure (22–24), raising the possibility of metabolically active subpopulations. The suite of analytical procedures used in this study could not directly discern for the presence of aqueous microlayers or *in situ* metabolism. Nonetheless, the successful PCR amplification of 1.5-kb 16S rDNA amplicons from EME-98-12 community DNA, for which the average size was ≈210 bp, suggests that our 16S rDNA reconstruction may reflect a metabolically active subset of the encased bacterial population or at least those capable of preferential protection of genomic DNA by an unknown mechanism.

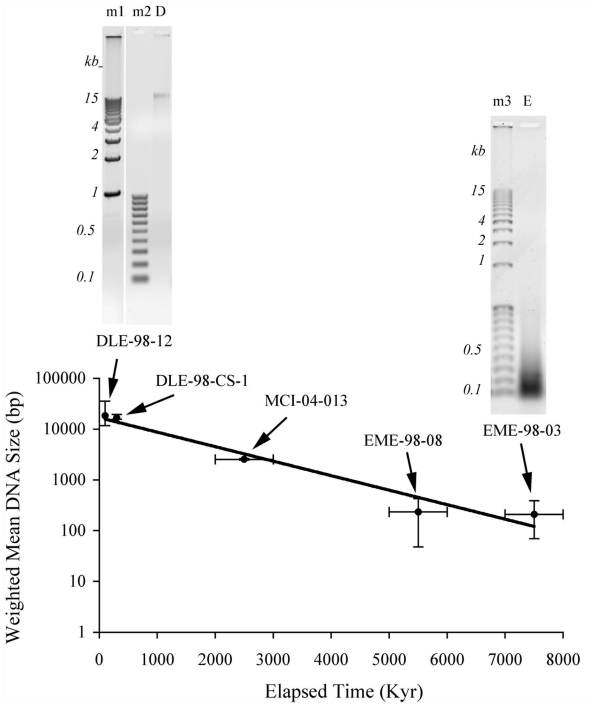

Fig. 4. Time-dependent DNA degradation curve for ice samples collected in Beacon and Mullins Valleys. The weighted mean DNA size was calculated from densitometry profiles of total extracted community DNA after gel electrophoresis. The weighted mean distance of the DNA peak was converted to size by using a distance-size calibration from molecular weight standards. Representative images of community DNA from DLE-98-12 and EME-98-03 are provided above their respective data points, illustrating the dramatic differences in DNA size. Error bars represent standard deviation of DNA size and ice age. Curve fit is based on an exponential regression ($y = 16804e^{-0.0007x}$, $r^2 = 0.96$).

To further evaluate the molecular composition of genes within the two ice samples, we constructed and sequenced through a BAC library containing partially BamHI-digested DLE-98-12 community DNA ($n = 132$) and an undigested end-repaired shotgun library containing EME-98-03 community DNA ($n = 427$). Although a significant proportion (39.4% for DLE-98-12 and 45.9% for EME-98-03) of the sequences in both samples had no annotated orthologs in GenBank, the remaining sequences encompassed a highly diverse set of extant functional genes (Fig. 5*A*). These included genes for DNA replication, transcription and translation, energy transduction, carbohydrate and lipid metabolism, cell motility and antibiotic resistance, among others. An overwhelming majority (>93%) of sequences in both libraries were derived from the *Bacteria* domain. *Actinobacteria*, *Proteobacteria*, and *Firmicutes* phyla, respectively, accounted for 52.6%, 27.2%, and 8.8% of the BLASTx matches in EME-98-03, supportive of superior DNA survival by bacteria, especially *Actinobacteria* (25). Although the relative frequencies of functional gene groups may change with a more extensive sequencing of the libraries, our analysis demonstrates that remnants of diverse recognizable metabolic genes and numerous ORFs of unknown function persist intact within ancient ice.

What could cause the relatively high fraction of the community genomes that have no known orthologs? One possibility is these are previously undiscovered genes not represented in the global database. The recent Global Ocean Sampling Expedition covering the Northwest Atlantic to the Eastern Tropical Pacific found that 85% of the assembled and 57% of the unassembled sequence data were unique at a 98% sequence cutoff (26), illustrating that the current database lacks an accurate representation of environmental sequences. A second possibility is that small fragment query size, due to DNA degradation, introduced an analysis artifact, preventing statistically significant BLASTx comparisons with homologous orthologs in the database. A majority of sequence query lengths for EME-98-03 were <300 bp, compared with >600 bp for DLE-98-12 (Fig. 5*B*), with the latter values reflecting partial insert size due to constraints on Sanger sequencing read lengths. Such a scenario implies a correlation between query length and e-value score, which was not found in either sample (Fig. 5*B*). Rather, we obtained a more random pattern, where a subset of small fragments frequently had high homology with extant genes, and others returned "no hit" from the National Center for Biotechnology Information database, implying they are rare genes.

The community DNA immobilized in Antarctic ice is essentially a "gene popsicle," which can potentially be acquired by extant organisms upon thawing (27, 28). Given the widespread influence of lateral gene transfer (LGT) within microbial populations and its putative influence on the tempo of microbial evolution (29, 30), one can envision periods in Earth's history when large numbers of ancient genes became available as ice sheets melted. Indeed, the tempo of evolution after major global glaciations appears to have increased dramatically (31), although causal mechanisms have been poorly defined. The vast majority of the ice on the Antarctic continent is <1 Ma; release of the microbes and DNA from such ice into the environment could potentially influence microbial genome content and structure. Although the ice volume for older formations is relatively small, the DNA in ≈8-Ma ice contains identifiable genetic information that potentially can be incorporated and used by microbes. Our analysis suggests that melting of polar ice in the geological past may have provided a conduit for large-scale phage-independent LGT, potentially scrambling microbial phylogenies and accelerating the tempo of microbial evolution. Finally, the preservation of microbes and their genes in icy comets may have allowed transfer of genetic material among planets. However, given the extremely high cosmic radiation flux in space, our results suggest it is highly unlikely that life on Earth could have been seeded by genetic material external to this solar system.

Materials and Methods

Sample Processing. Ice samples were obtained by removing ≈20–75 cm of thick debris and the top ≈15 cm of the buried glacier and cutting out a square block ≈20 cm on a side (6). The 0°C isotherm reaches a maximum depth of ≈15 cm in the region; the ice samples we analyzed were from well below this depth (35-cm depth minimum). Samples were triple wrapped in plastic bags and stored at −20°C until processing. Ice samples were processed by using a surface decontamination and melting procedure consistent with previous studies (1, 32, 33). A section of block ice (≈1 kg) was removed from −80°C and equilibrated at −20°C for at least 24 h to minimize cracking. Ice was soaked in ice-cold 95% ethanol for 1 min, followed by extensive rinsing with 0.22 μm-filtered MilliQ water, effectively ablating the exterior ≈3-cm shell of ice samples (corresponding to ≈300 ml or ≈30% of total ice volume). These procedures were effective at removing surface contamination from inner shell ice samples (32, 33). The decontaminated interior ice was thawed in a sterile Whirl-Pak (Nasco, Fort Atkinson, WI) plastic bag at 4°C and used for analyses. To control for laboratory contamination, 1 liter of MilliQ rinse water was frozen, thawed, filtered onto polycarbonate (PC) filters, and subjected to identical analytical procedures. All procedures were performed by using bleach-sterilized work areas, a UV-irradiated laminar flow hood, ethanol-flame sterilized tools, laboratory coats, and sterilized gloves.

Chemical Analyses. Assays for dissolved inorganic nitrogen (NH_4^+, NO_2^-, and NO_3^{-2}) and soluble reactive phosphate were performed by Lachat QuickChem AE Elemental Analyzer (Lachat Instruments, Milwaukee, WI). Determinations of dissolved organic car-

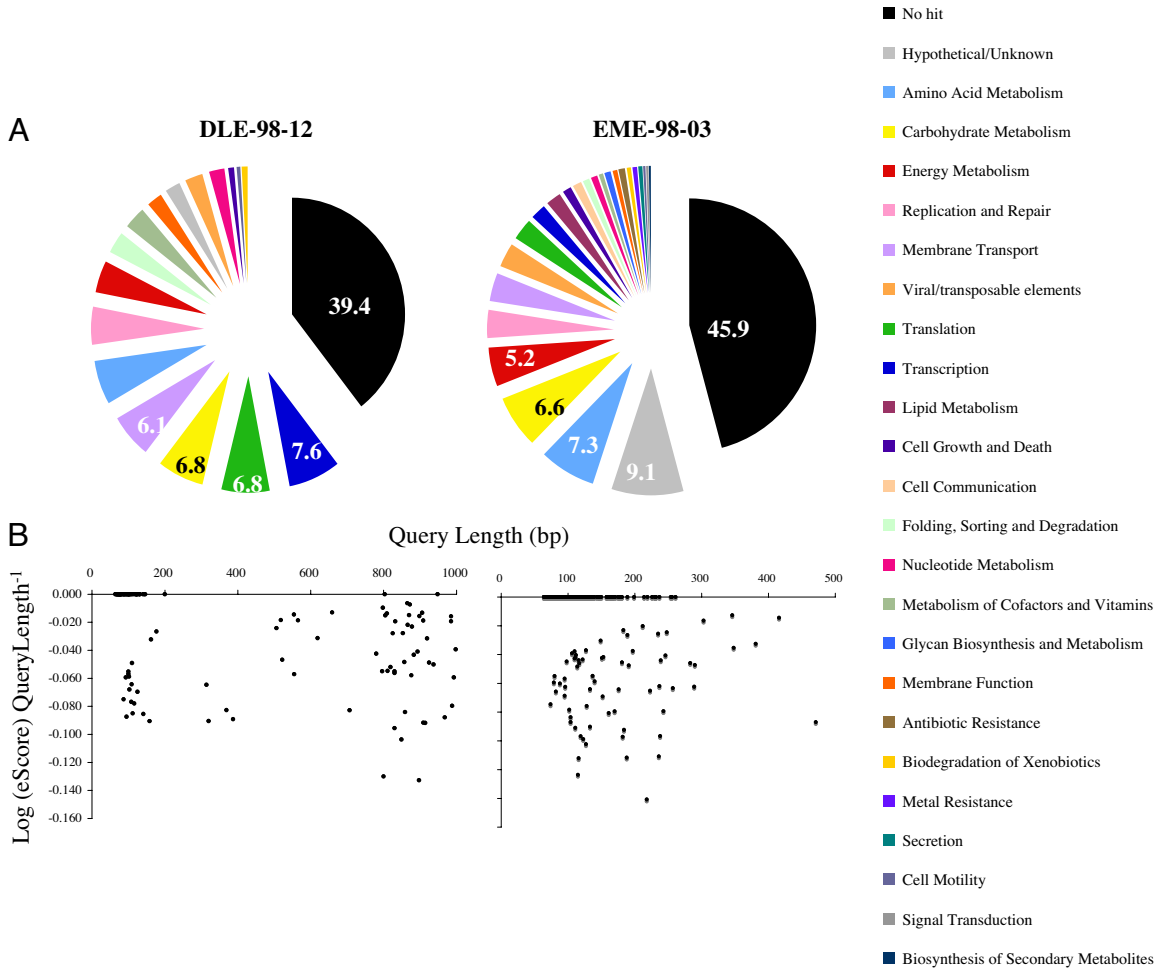

Fig. 5. The genetic content of community ice DNA from DLE-98-12 and EME-98-03. (*A*) The distribution of gene categories for a random sampling of BAC (DLE-98-12; $n = 132$ sequences) and end-repaired (EME-98-03; $n = 427$ sequences) clone libraries, as determined by BLASTx analysis. A majority (≈55–60%) of the sequences from both ice sources had BLASTx matches to a wide variety of metabolic genes (key), whereas others (≈40–45%) had no statistical similarity to sequences in GenBank below the 10^{-5} e-value cutoff. The contribution (%) for the top five categories is given. A complete representation for all categories is provided in SI Table 5. (*B*) An analysis of the impact of sequence query size on the statistical similarity to sequences in GenBank (e-score). The log (e-score) per unit query length as a function of query length was plotted for each recovered ice sequence. Sequences with no BLASTx hit are distributed along the *x* axis.

bon were done on a Shimadzu (Columbia, MD) TOC-5000A analyzer. Total dissolved N was analyzed by Antek (Houston, TX) Model 7000B, using a high-temperature combustion followed by chemiluminescent detection of nitric oxide.

Epifluorescence and Scanning Electron Microscopy. Meltwater was preserved in 0.2 μm-filtered 2% formalin and stored at 4°C until processed (within 1 week). Cell enumeration was by a modified SYBR gold (Molecular Probes, Invitrogen, Carlsbad, CA) staining procedure, whereby SYBR gold (1×) was added directly to preserved aliquots (15 min; dark), followed by filtering onto 0.22-μm black PC track-etched membrane filters and visualization at ×1,000 on a Zeiss (Peabody, MA) Axioskop. At least 300 cells were counted for 30 random fields. For SEM analysis, meltwater was collected onto sterile 0.22-μm PC filters, preserved in Trump's fixative, rinsed in 0.2 μm-filtered 50 mM phosphate buffer and MilliQ water, followed by a stepwise ethanol dehydration, coating with gold palladium, and SEM visualization.

DNA Extraction and PCR Amplification. Meltwater was centrifuged in acid-cleaned sterilized bottles (15,000 × *g*; 20 min; 4°C) to pellet sediment particles. The supernatant was vacuum filtered onto autoclaved 0.2-μm PC filters using a sterilized filtration manifold. Filters and sediment were immediately frozen until analysis. DNA was extracted from both the filters and sediment using the Soil-Master kit (Epicentre, Madison, WI) according to manufacturer's instructions, pooled, and stored in TE buffer (10 mM Tris·HCl, pH 7.8/1 mM EDTA) at −80°C. Extraction procedures were identical for all ice samples and used minimal vortexing to minimize shearing. The size and integrity of total extracted community DNA were determined by agarose gel electrophoresis (0.8%) followed by staining with 1× SYBR gold and visualization using a Typhoon 9400 Variable Mode Imager equipped with ImageQuant Solutions software (Amersham Biosciences, Piscataway, NJ). The weighted mean DNA size (in basepairs) was calculated from densitometry profiles and a migration-size calibration curve with molecular weight standards using ImageJ 1.34s software (National Institutes of Health, Bethesda, MD).

Bacteria, Archaea, and Eukaryotic. Specific primers were used to amplify 16S rDNA genes in ice community DNA, as described (34, 35). PCR was optimized by both diluting the template (>10-fold) and by increasing the number of thermal cycles. To control for false-positive PCR signals, 1 liter of MilliQ water was frozen, thawed, filtered on a PC filter, and subjected to the same DNA extraction procedure. This material was used as a template with the *Bacteria*-specific primers to test for contamination and PCR artifacts.

Generation of Clone Libraries. 16S rDNA PCR amplicons were cloned (TOPO TA Cloning vector; Invitrogen, Carlsbad, CA) and plasmid DNA (118 EME clones, 140 DLE clones) was bidirectionally sequenced. Chimeric sequences were identified with the CHIMERA-CHECK program (Ribosomal Database Project II, Michigan State University, East Lansing, MI) and discarded. Sequences with >98% identity were grouped together and selected for full-length sequencing. The robustness of phylogenetic tree branching order was tested through analyses using different portions of each 16S rDNA sequence. 16S rDNA sequences correspond to GenBank accession nos. EF127594–EF127627.

The BAC library was generated for DLE-98-12 by ligating BamH1-digested community DNA into a copy-control pCC1BAC vector (Epicentre). For EME-98-03, end-repaired community DNA was ligated into the blunt cloning-ready Copy Control pCC1 Vector (Epicentre). Clones were grown on Luria Broth under chloramphenicol selection. Colonies on agar plates, frozen ligation reactions, and frozen glycerol stocks of transformants were hand-delivered on dry ice to the Microbial Genomics group at The Institute for Genomic Research (TIGR) for sequencing. Metagenomic sequences correspond to GenBank accession nos. ER915562–ER916113.

Analysis of Metabolic Activity. Sixty-milliter aliquots of meltwater samples were transferred into acid-cleaned sterile glass Erlenmeyer flasks. Aliquots were spiked with either 6.78 μCi ^{3}H-thymidine (specific activity = 1.13 Ci/mmol; 1 Ci = 37 GBq) or 9.12 μCi ^{3}H-leucine (specific activity = 1.13 Ci/mmol). Because of different background deoxycholate concentrations in DLE-98-12 and EME-98-03 meltwaters (SI Table 1), 2.4 and 0.68 μCi of ^{14}C-glucose were added, respectively, corresponding to 0.7 and 0.2 μM. Labeled samples were dispensed (3 ml) into acid-washed sterile 10-ml glass Erlenmeyer flasks (Kimble/Kontes, Vineland, NJ), fitted with a gas-tight stopper and a sterile plastic center well (Kimble/Kontes) with a fluted-filter paper wick. Formalin-killed controls (0.2 μm-filtered; 2% final concentration) were used to correct for abiotic transformation and incorporation onto particles. MilliQ rinse water was used to test for contamination artifacts during sample processing. All samples were incubated at 4°C in the dark.

Triplicate samples were processed for ^{3}H-leucine, ^{3}H-thymidine and ^{14}C-incorporation. All reactions were terminated with 2% formalin. After addition of 5% trichloroacetic acid (TCA), ^{3}H-thymidine flasks were incubated on ice for 15 min, and ^{3}H-leucine flasks were heated at 80°C for 15 min. The entire sample was then collected onto 0.45-μm pore-size mixed cellulose membrane filters using a sterile syringe and a Luer-lock Swinnex (Millipore) filter housing. Filters were rinsed with 1 ml of ice-cold 5% TCA (2×) and with 1 ml of 80% ice-cold ethanol (3×) before dissolving in ethyl acetate and liquid scintillation counting.

For ^{14}C-measurements, the wick was wetted with β-phenethylamine and meltwaters were acidified with 100 μl of 5 M H_2SO_4. Samples were incubated overnight at room temperature for passive distillation of ^{14}C-CO_2 onto the β-phenethylamine soaked wicks, which were removed for liquid scintillation counting (LSC). Acidified meltwater samples were collected onto 0.22 μm pore-size PC filters, rinsed with sterile, 0.22 μm filtered MilliQ water (3×), and dissolved in ethyl acetate for LSC.

Recovery of Viable Microorganisms. Ice-melt water was amended with nutrients and incubated at 4°C in the dark. Nutrient formulations were as follows in g·liter^{-1} (*T1*, 5 g of peptone, 0.15 g of ferric ammonium citrate, 0.2 g of $MgSO_4 \cdot 7H_2O$/0.05 g of $CaCl_2$/0.05 g of $MnSO_4 \cdot H_2O$/0.01 g of $FeCl_3 \cdot 6H_2O$ 0.01; *T2*, 1 g of glucose/1 g of peptone/0.5 g of yeast extract/0.2 g of $MgSO_4 \cdot 7H_2O$/0.05 g of $MnSO_4 \cdot 4H_2O$; *T3*, 1 g of glucose/0.5 g of casamino acids/0.5 g of yeast extract/1 g of KH_2PO_4/0.5 g of $CaCl_2 \cdot 2H_2O$/0.5 g of $MnCl_2 \cdot 4H_2O$; *T4*, R2A). All nutrient formulations were made as concentrated stocks (20–200×), sterilized by autoclaving, and directly added (<1/50 volume ratio) to meltwater at 1× final concentration. Growth was monitored by optical density (600 nm) and epifluorescence microscopy. Blanks consisted of autoclaved MilliQ water amended with the same nutrients. Subsamples were removed for PCR amplification of 16S rDNA using previously mentioned primers and for plating onto solid media. Nested PCRs used community 16S rDNA amplicons or isolate genomic DNA as templates and used signature 16S rDNA primer sequences (Arose-232F: 5′-GAATTTTGGTTTTGGATGGACTCGC-3′ and Arose-1008R: 5′-TGTCTCCAGGTGTTTCCAGTCC-3′ were specific to DLE011i and *A. roseus* CMS90; Arthro-486F: 5′-GACATTCCACGTTTTCCGCG-3′ and Arthro-1286R: 5′-CTCCACCTCACAGTATCGCAAC-3′ were for all *Arthrobacter* sp.).

We thank John Heidelberg and Bill Nelson at The Institute for Genomic Research (TIGR) for assistance with metagenomic sequencing and analysis. We also thank Ron Lauck and Sybil Seitzinger for the chemical analyses; Felisa Wolfe-Simon and Costantino Vetriani for help with the phylogenetic analyses; Valentin Starovoytov for SEM analysis; and Jörg Schäfer, Carl Swisher, and Gordon Thomson for helpful discussions on cosmic fluxes in Beacon Valley ice. This study was supported by the Gordon and Betty Moore Foundation (K.D.B. and P.G.F.), the U.S. National Science Foundation (Grant ANT-0338291, to D.R.M.), and the Korea Antarctic Research Program (Grants PP-04104 and PP-05001).

1. Karl DM, Bird DF, Björkman K, Houlihan T, Shackelford R, Tupas L (1999) *Science* 286:2144–2147.
2. Priscu JC, Fritsen CH, Adams EE, Giovannoni SJ, Paerl HW, McKay CP, Doran PT, Gordon DA, Lanoil BD, Pinckney JL (1998) *Science* 280:2095–2098.
3. Christner B, Mosley-Thompson E, Thompson LG, Zagorodnov V, Sandman K, Reeve JN (2000) *Icarus* 144:479–485.
4. Rignot E, Hallet B, Fountain A (2002) *Geophys Res Lett* 29:10.1029/2001/GL013494.
5. Schäfer J, Baur H, Denton GH, Ivy-Ochs S, Marchant DR, Schlüchter C, Wieler R (2000) *Earth Planet Sci Lett* 179:91–99.
6. Marchant DR, Lewis AR, Phillips WM, Moore EJ, Souchez RA, Denton GH, Sugden DE, Potter N, Jr, Landis GP (2002) *GSA Bull* 114:718–730.
7. Sugden DE, Marchant DR, Potter N, Souchez RA, Denton GH, Swisher CC, Tison JL (1995) *Nature* 376:412–414.
8. Pearce DA (2003) *Microb Ecol* 46:92–105.
9. Säwström C, Mumford P, Marshall W, Hodson A, Laybourn-Parry J (2002) *Polar Biol* 25:591–596.
10. Brinkmeyer R, Knittel K, Jürgens J, Weyland H, Amann R, Helmke E (2003) *Appl Environ Microbiol* 69:6610–6619.
11. Carpenter EJ, Lin S, Capone DG (2000) *Appl Environ Microbiol* 66:4514–4517.
12. Holt JG, Krieg NR, Sneath PHA, Staley JT, Williams ST (1994) *Bergey's Manual of Determinative Bacteriology* (Williams and Wilkins, Baltimore).
13. Rogers SO, Ma L-J, Zhao Y, Theraisnathan V, Shin S-G, Zhang G, Catranis CM, Starmer WT, Castello JD (2005) in *Life in Ancient Ice*, eds Castello JD, Rogers SO (Princeton Univ Press, Princeton, NJ), pp 5–21.
14. Reddy GS, Prakash JS, Matsumoto GI, Stackebrandt E, Shivaji S (2002) *Int J Syst Evol Microbiol* 52:1017–1021.
15. Muñoz J, Felicísimo AM, Cabezas F, Burgaz AR, Martínez I (2004) *Science* 304:1144–1147.
16. Sambrotto R, Burckle L (2005) in *Life in Ancient Ice*, eds Castello JD, Rogers SO (Princeton Univ Press, Princeton, NJ), pp 94–105.
17. Willerslev E, Hansen AJ, Poinar HN (2004) *Trends Ecol Evol* 19:141–147.
18. Eigen M, deMaeyer L (1958) *Proc R Soc London A* 247:505–533.
19. Lindahl T (1993) *Nature* 362:709–715.
20. Lemaitre G, Vallarta MS (1933) *Phys Rev* 43:87–91.
21. Gosse JC, Phillips FM (2001) *Q Sci Rev* 20:1475–1560.
22. Anderson DM, Tice AR (1973) in *Ecological Studies* (Springer, New York), Vol 4, pp 107–124.
23. Jepsen SM (2005) PhD thesis (Montana State Univ, Bozeman).
24. Price PB (2007) *FEMS Microbiol Ecol* 59:217–231.
25. Willerslev E, Hansen AJ, Rønn R, Brand TB, Barnes I, Wiui C, Gilichinsky D, Mitchell D, Cooper A (2004) *Curr Biol* 14:R9–R10.
26. Rusch DB, Halpern AL, Sutton G, Heidelberg KB, Williamson S, Youseph S, Wu D, Eisen JA, Hoffman JM, Remington K, *et al.* (2007) *PLoS Biol* 5:398–431.
27. Castello JD, Rogers SO (2005) in *Life in Ancient Ice*, eds Castello JD, Rogers SO (Princeton Univ Press, Princeton, NJ), pp 289–300.
28. Rogers SO, Starmer WT, Castello JD (2004) *Med Hypoth* 63:773–777.
29. Koonin EV, Makarova KS, Aravind L (2001) *Annu Rev Microbiol* 55:709–742.
30. Ochman H, Lawrence JG, Groisman EA (2000) *Nature* 405:299–304.
31. Knoll AH (2003) *Life on a Young Planet: The First Three Billion Years of Evolution on Earth* (Princeton Univ Press, Princeton, NJ).
32. Christner BC, Mikucki JA, Foreman CM, Denson J, Priscu JC (2005) *Icarus* 174:572–584.
33. Rogers SO, Theraisnathan V, Ma LJ, Zhao Y, Zhang G, Shin S-G, Castello JD, Starmer WT (2004) *Appl Environ Microbiol* 70:2540–2544.
34. Lane DJ (1991) in *Nucleic Acid Techniques in Bacterial Systematics*, eds Stackebrandt E, Goodfellow M (Wiley, New York), pp 115–175.
35. DeLong EF (1992) *Proc Natl Acad Sci USA* 89:5685–5689.